Structure of low-lying states in ^{94}Mo

E. Adamides, L. D. Skouras, and A. C. Xenoulis
Tandem Accelerator Laboratory, NRC "Demokritos", Aghia Paraskevi-Attikis, Greece
(Received 30 June 1980)

The $(p,p'\gamma)$ reaction has been used to investigate the structure of low-lying states in ^{94}Mo. Single directional correlations provided reliable branching ratios, J^π assignments, and multipole mixing ratios from analysis of the correlations via the compound statistical theory for nuclear reactions. From these measurements the J^π value of the 2067.1 keV level was definitely assigned as 2^+. Lifetimes for two states in ^{94}Mo and limits for two additional states were obtained by the Doppler-shift-attenuation method. Values of $B(M1)$ and $B(E2)$ were obtained for six transitions in ^{94}Mo. Futhermore, properties of low-lying states in ^{94}Mo were calculated in the shell-model framework and are compared with the corresponding experimental quantities.

[NUCLEAR REACTIONS ^{94}Mo$(p,p'\gamma)$, E_p=4.8 and 5.0 MeV, enriched targets. Measured $E_\gamma, I_\gamma(\vartheta)$, $\Delta E\gamma(\tau)$, deduced ^{94}Mo levels, branching ratios, τ, $\delta(E2/M1)$, $B(E2)$, $B(M1)$; Ge(Li) detectors. Calculated ^{94}Mo positive-parity levels, $B(E2)$, $B(M1)$, τ, branching ratios.]

I. INTRODUCTION

Properties of electromagnetic transition from high-spin states in ^{94}Mo were recently reported and compared with shell-model predictions.[1] In these calculations, while full configuration mixing was assumed for the two valence neutrons occupying any of the $1d_{5/2}$, $2s_{1/2}$, $1d_{3/2}$, and $0g_{7/2}$ orbitals, only the $0g_{9/2}$ orbital was considered for the two valence protons. Multipole mixing ratios thus determined were not only close to the observed ones in magnitude,[1] but they also predicted correctly the sign of δ, which is a very sensitive criterion on the wave functions. It should be noted, however, that the validity of the employed model space cannot be tested fully before a comparison with the properties of low-spin states give equally satisfactory agreement.

In the present study, calculated properties of electromagnetic transitions and transition probabilities from low-spin states in ^{94}Mo are compared with the corresponding experimental quantities. For the latter we have measured mixing ratios of transitions and lifetimes of low-lying states in ^{94}Mo utilizing spectrometry of prompt γ rays emitted in the reaction ^{94}Mo$(p,p')^{94}$Mo$^*(\gamma)$.

Previous relevant experimental information has been obtained by $\gamma\gamma$-angular correlation measurements following the decay of the 2^+ isomeric state in the ^{94}Tc isotope,[2] and via multipole Coulomb excitation.[3]

II. EXPERIMENTS AND RESULTS

The proton beams were provided by the $T11/25$ Tandem Van de Graaff accelerator of the NRC "Demokritos." The targets employed were self-supporting foils, 3 mg/cm^2 thick, of molybdenum metal enriched to 94.6% in mass 94, which were prepared by rolling of the metal. For γ ray counting, a high-resolution 18% Ge(Li) detector which had a full width at half maximum (FWHM) of 1.9 keV at 1332 keV was used. Standard electronics were employed for the accumulation of spectra over 4096 channels in a PDP-11/15 on-line computer. Angular distributions and Doppler shifts of single γ rays following the reaction ^{94}Mo(p,p') ^{94}Mo$^*(\gamma)$ were measured at 4.8 and 5.0 MeV bombardment energy, respectively. Higher bombarding energies were avoided, since γ rays from the decay of ^{94}Tc, produced in the reaction ^{94}Mo(p,n) ^{94}Tc ($Q=-5.1$ MeV), strongly interferred with the $(p,p'\gamma)$ reaction. In order to ensure the applicability of the statistical theory in the ^{94}Mo $(p,p')^{94}$Mo$^*(\gamma)$ reaction, the proton bombarding energy in the distribution measurements was chosen at 4.8 MeV in order to avoid the excitation of analog states[4] in the compound nucleus.

Four low-lying states, at 871.1 (2_1^+), 1573.6 (4_1^+), 1863.9 (2_2^+), and 2067.1 keV (2_3^+), were sufficiently excited at 4.8 MeV bombardment energy to permit the investigation of their deexciting transitions.

A. Angular distributions

Spins of levels and multipole mixing ratios of electromagnetic transitions were obtained from angular distribution measurements at 4.8 MeV bombarding energy. Singles γ-ray spectra were taken at six detector angles $\Theta_d=0°$, 30°, 45°, 55°, 70°, and 90° with respect to the incident proton beam. The normalization of the spectra was carried out with the help of high intensity peaks in the associated spectrum of a fixed Ge(Li) monitor. The obtained angular distributions were first analyzed by a least-square fit of the data to the

function

$$W(\Theta_d) = A_0[1 + A_2 P_2(\cos\Theta_d) + A_4 P_4(\cos\Theta_d)]. \quad (1)$$

The coefficients of the Legendre polynomials obtained in this way were not corrected for solid angle since the latter was so small, 0.02 sr, that it essentially reduced the corresponding geometrical attenuation coefficients to unity. The experimental A_2 and A_4 coefficients are given in Table I. The angular distributions were further analyzed to extract δ values. For that purpose the Hauser-Feshbach theory[5] for nuclear reactions was applied. The evaluation of the theoretical distributions was performed with the program MANDY (Ref. 6) which was modified in order to fit the theoretical distribution to the experimental $W(\Theta_d)/A_0$ data and yield an approximate χ^2 as a function of δ. Transmission coefficients for protons were obtained from the penetrability tables of Mani *et al.*[7] The distributions were further analyzed with the program MINUIT (Ref. 8), which was modified in this laboratory, in a search for a precise minimum χ^2 in which a step in δ of 0.001 was used. The theoretical A_2 and A_4 coefficients are given in Table I below the corresponding experimental quantities. Initial spin values in the range permitted by its mode of decay were considered only for the 2067.2-keV level, the definite 2^+ assignment of which has been challenged in a previous study.[9] The minimum χ^2 value divided by the degrees of freedom and the corresponding δ value at the minimum are contained in the fourth and fifth columns of Table I. The uncertainties quoted with the present δ value refer to the 68.3% confidence limit and are evaluated according to the procedure prescribed by Rogers.[10] The mixing ratio is defined in terms of emission matrix elements according to Krane and Steffen.[11] In the last column of Table I the proposed δ value is contained, which has been selected according to criteria delineated below.

As can be seen in Fig. 1, the distribution of the 1196.0-keV transition establishes a definite 2^+ assignment to the 2067.1-keV level. The δ values obtained for the 871.1- and 702.6-keV γ rays are zero (within the experimental error), indicating pure $E2$ transitions, as expected.

B. Lifetime measurements

Lifetimes for two levels in ^{94}Mo and lower limits for two others were obtained from Doppler-shift attenuation measurements. Singles spectra were measured at eight angles $\Theta_d = 0°$, 30°, 45°, 55°, 70°, 90°, 110°, and 130° with respect to the beam direction. Due to the low initial recoil velocity, the observed shifts are very small. In order to obtain accurate results for the centroid positions of the γ rays in these experiments, care was paid in keeping the proton current low and steady to avoid rapid changes in the energy stability of the system.

TABLE I. Summary of angular distribution analysis.

Transition (keV) $J_i^\pi \to J_f^\pi$	A_2 Experimental[a]	A_2 theoretical	A_4 Experimental[a]	A_4 theoretical	χ^2	Present	Previous	Proposed
871.1 → 0	0.302	9	−0.118	9				
$2^+ \to 0^+$	0.292		−0.149		2.1	$E2$		$E2$
1573.6 → 871.1	0.318	33	0.005	34				
$4^+ \to 2^+$	0.371		−0.071		1.9	0.02 ± 0.03		$E2$
1863.9 → 871.1	−0.230	25	−0.026	25				
$2^+ \to 2^+$	−0.230		−0.021		1.6	$-0.87^{+0.09}_{-0.17}$	−0.044[b]	$-0.87^{+0.09}_{-0.17}$
or	−0.232		−0.043		1.7	$-3.2^{+0.7}_{-0.9}$	$-2.00^{+0.25}_{-0.35}$[c]	
2067.1 → 871.1	0.523	50	0.051	51				
$0^+ \to 2^+$	0.000		0.000		29			
$1^+ \to 2^+$	0.048		0.000		24			
$2^+ \to 2^+$	0.439		−0.013		1.4	$0.62^{+0.21}_{-0.15}$		$0.62^{+0.21}_{-0.15}$

[a] The underlined numbers are estimated uncertainties referring to the last quoted significant figures.

[b] Reference 12.

[c] Reference 2.

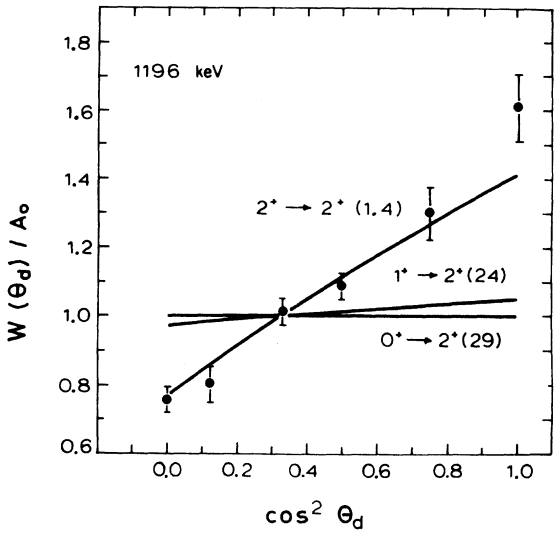

FIG. 1. Singles angular distribution of the 1196.0-keV γ ray. The solid lines are theoretical correlations for the δ value that gave the minimum χ^2 value indicated in parentheses after the spin sequence shown.

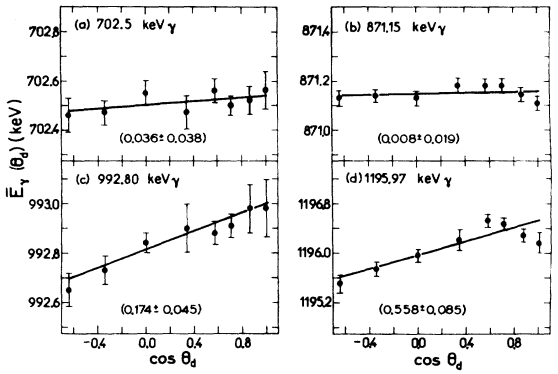

FIG. 2. Plots of the centroid energy in keV for the indicated γ rays from ^{94}Mo observed in singles measurements vs $\cos\Theta_d$. The numbers in parentheses are the least-square slopes for the straight line fit to the data.

The theoretical average attenuation factors $\bar{F}(\tau)$ have been calculated by averaging the attenuation factor $F(\tau)$ over all initial velocities of the recoil nucleus employing the angular correlation function as a weighing factor, according to the formalism of Moazed *et al.*[13] In the evaluation of the recoil velocity as a function of time, the stopping power theory of Lindhard *et al.*[14] as modified by Blaugrund[15] was used. In the calculation of the stopping power, the generally adopted expression

$$T_t = f_e T_e + f_n T_n \tag{2}$$

was used, where T_t is the total stopping power, e and n refer to the electronic and nuclear stopping powers, and f_e and f_n are adjustable parameters. In this work, $f_e = f_n = 1$ was assumed.

The observed photopeak centroid energy has been plotted in Fig. 2 as a function of $\cos\Theta_d$ together with the least-square fitted lines. The observed Doppler shift, given by the slope of the line, is indicated in parentheses. The experimental $\bar{F}(\tau)$ values and the extracted lifetimes are shown in Table II. In these results, feeding from above was not considered, since it is very weak relative to the direct population. The quoted uncertainties are only statistical. In Table II are also shown the lifetimes as determined by multipole Coulomb excitation reported in Ref. 3. For the first two excited states, for which only lifetime limits were obtained here, the previous values were adopted.

The present and previous values for the lifetime of the 1863.9-keV level do not overlap within the experimental errors. It should be noted, however, that this lifetime in Ref. 3 was evaluated assuming a multipole mixing ratio for the 992.8-keV transition $\delta = -2.00^{+0.25}_{-0.35}$ taken from Ref. 2, while here the lifetime of the 1863.9-keV level was determined directly from the Doppler-shift-attenuation (DSA) measurements. Moreover, this lifetime reevaluated from the $B(E2)$ value of Ref. 3 and the δ value determined in the present work

TABLE II. Lifetime for levels in ^{94}Mo determined via the DSA method from centroid shifts and comparison with other available data.

Level (keV)	Transition (keV)	$\tilde{F}(\tau)$[a]	T level (ps) Present	Coulomb exc.[b]	Adopted
871.1	871.1	0.009 20	≥1.3	3.7 ±0.2	3.7 ±0.2
1573.6	702.5	0.048 50	≥0.3	7.1 ±1.0	7.1 ±1.0
1863.9	992.8	0.156 48	$0.185^{+0.095}_{-0.043}$	0.53 ±0.13	$0.185^{+0.095}_{-0.043}$
2067.1	1196.0	0.432 66	$0.046^{+0.014}_{-0.007}$		$0.046^{+0.014}_{-0.007}$

[a] The underlined numbers are estimated uncertainties referring to the last quoted significant figures.

[b] Reference 3.

overlaps, within the experimental uncertainties, with the one measured here.

III. REDUCED TRANSITION PROBABILITIES

From the branching ratios, multipole mixing ratios, and the level lifetimes measured in the present study, the reduced transition probabilities $B(E2)$ and $B(M1)$ for the electric quadrupole and the magnetic dipole components of six transitions in ^{94}Mo were deduced. These values are summarized in the last two columns of Table III. The $B(E2)$ and $B(M1)$ values are given in Weisskopf units (W.u.) and were calculated via the procedure described in the Appendix of Ref. 16. In Table IV we show the $B(E2)$ values for the 992.8-keV transition calculated from the currently determined lifetime of the corresponding 1863.9-keV level and four different δ values of the 992.8-keV transition currently and previously[2,12] determined. A comparison of these results with the $B(E2)$ value determined via Coulomb excitation[3] helps to select a unique δ value for the 992.8-keV transition, $\delta = -0.87^{+0.09}_{-0.17}$, which is the only reproducing, within the experimental error, the value $B(E2) = 45 \pm 10$ reported in Ref. 3.

IV. COMPARISON WITH THEORY

In this section we compare the present experimental results on the electromagnetic decay of the low-lying states of ^{94}Mo with the predictions of two shell-model calculations. These two calculations (to be hereafter distinguished as 1 and 2) differ in the choice of the model space and also in the manner in which they estimate the appropriate effective interaction.

In calculation 1 a $^{90}_{40}$Zr core is assumed and the two valence protons of ^{94}Mo are considered to be in the $0g_{9/2}$ orbital, while the two additional neutrons are distributed among the close-spaced $1d_{5/2}$, $2s_{1/2}$, $1d_{3/2}$, and $0g_{7/2}$ orbitals.[17] The effective two-body interaction was calculated to second order[18] employing the "Sussex" interaction[19] as bare G matrix, while the single-particle energies were taken from experiment.[20] It should be noted that the results of calculation 1 have been found to describe satisfactorily a number of structural features of the low-lying states of ^{94}Mo.[1,17]

To perform calculation 2 we have assumed a ^{88}Sr core and distributed the four valence protons in the $1p_{1/2}$ and $0g_{9/2}$ orbitals. On the other hand, the two valence neutrons were restricted to be in the $1d_{5/2}$ and $2s_{1/2}$ orbitals. The effective Hamiltonian for this choice of the model space has been estimated by a least-square fit to the observed levels of several nuclei in the mass 90 region.[21,22]

The calculated excitation energies of levels with J^π values of 0^+, 2^+, and 4^+ are shown in Fig. 3 in comparison with experiment.[23] As may be seen from Fig. 3, the spectrum obtained with calculation 2 is in satisfactory agreement with experiment. A similar agreement is also observed in the results of calculation 1 apart for the cases of the second 0^+ and of the fourth 2^+ states which are calculated to be at too high an excitation in comparison to the experiment. Such a feature clearly suggests that these two states are composed predominantly by configurations which are outside the model space used in calculation 1.

In our calculation of the electromagnetic transitions of the ^{94}Mo levels, we have employed effective operators for both the $M1$ and $E2$ modes of decay. In the calculation of $E2$ rates the proton and neutron effective charges have been treated as parameters and the values that produce the best overall agreement with experiment have been chosen. It was found that for both calculations a proton effective charge of $2e$ is required, while the values deduced for the neutron effective charge are $1.6e$ and $2.4e$ for calculations 1 and 2, respectively.

A more realistic approach has been followed in

TABLE III. Summary of the electromagnetic properties of transitions in ^{94}Mo determined in this work.

Transition energy (keV)	$J^\pi_i \to J^\pi_f$	Branching %	$\delta(E2/M1)$	$B(E2)$ (W.u.)	$B(M1)$ (W.u.)
871.1	$2^+_1 \to 0^+_1$	100	$E2$	17.2[a]	
702.5	$4^+_1 \to 2^+_1$	100	$E2$	26.6[a]	
992.8	$2^+_2 \to 2^+_1$	92	$-0.87^{+0.09}_{-0.17}$	71^{+17}_{-39}	$0.09^{+0.02}_{-0.05}$
1863.9	$2^+_2 \to 0^+_1$	8	$E2$	$0.60^{+0.39}_{-0.48}$	
1196.0	$2^+_3 \to 2^+_1$	90	$0.62^{+0.21}_{-0.15}$	71^{+37}_{-33}	$0.26^{+0.05}_{-0.10}$
2067.1	$2^+_3 \to 0_1$	10	$E2$	$1.9^{+0.6}_{-0.9}$	

[a] Adopted from Ref. 3.

TABLE IV. $B(E2)$ values for the 992.8-keV transition calculated from the lifetime of the corresponding level measured here and the previously and currently reported δ values.

$\delta(E2/M1)$	$B(E2)$ (W.u.)
-0.044[a]	0.3
$-2.00^{+0.25}_{-0.33}$[b]	132^{+30}_{-66}
$-0.87^{+0.09}_{-0.17}$	71^{+17}_{-39}
$-3.2^{+0.7}_{-0.9}$	151^{+33}_{-74}

[a] Reference 12.
[b] Reference 2.

the evaluation of the $M1$ effective matrix elements. Thus, following the original idea of Arima and Horie,[24] we have estimated the first-order corrections to the bare $M1$ matrix elements. These corrections are presented diagrammatically in Fig. 4. From the graphs shown in Fig. 4, (a) and (b) represent one-body corrections, while (c)–(f) represent two-body corrections. Because of the selectivity of the $M1$ operator, the only contribution to graphs 4(a) and 4(b) arises when the particle p is a neutron in the $0g_{7/2}$ orbital while the hole h is a neutron in the $0g_{9/2}$ orbital. The matrix elements of the effective two-body $M1$ operator have been evaluated between proton and neutron

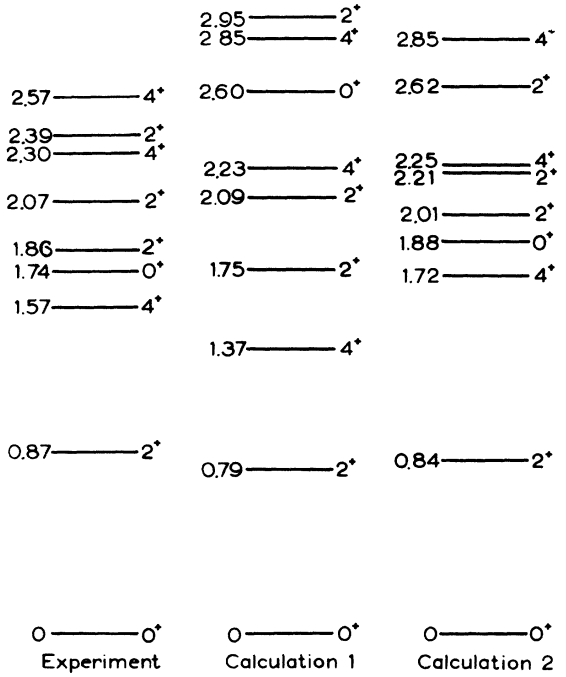

FIG. 3. Experimental and calculated spectra of the low-lying 0^+, 2^+, and 4^+ states of ^{94}Mo.

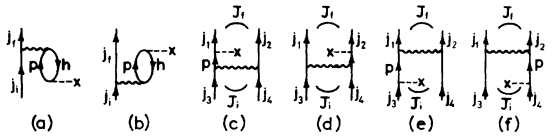

FIG. 4. First order graphs contributing to the $M1$ transitions of ^{94}Mo. See text for details.

configurations. In the first case, p in diagrams 4(c)–4(f) represents a proton in the $0g_{7/2}$ orbital, while in the second it represents a neutron in the $1d_{3/2}$ orbital. These restrictions to the values of p occur because the bare $M1$ operator connects only single-particle states with the same radial, n, and orbital angular momentum, l, quantum numbers. Since, as was previously discussed, the proton $0g_{7/2}$ is not included in the model spaces of calculations 1 and 2, the two-body corrections to the $M1$ matrix elements between proton states have been considered in both calculations. A different situation occurs, however, for the $M1$ matrix elements between neutron states. Here, as described above, the neutron $1d_{3/2}$ orbital is included in the model space of calculation 1 while it lies outside the model space of calculation 2. Thus the effects of graphs 4(c)–4(f) on the matrix elements of the $M1$ operator between neutron states have only been considered in calculation 2, since these effects are directly taken into account in calculation 1. The effects of the one-body graphs 4(a) and 4(b) are listed in Table V, while those of the two-body graphs 4(c)–4(f) are listed in Table VI. All corrections have been calculated using the Sussex interaction[19] and the single-particle energies of Ref. 20.

The calculated $B(M1)$ and $B(E2)$ values are listed in Table VII together with the experimental estimates. The $B(M1)$ values which have been calculated using the bare operator are also listed in Table VII so that one can easily check the overall effects produced by the renormalization pro-

TABLE V. Effects of the core polarization graphs on the $M1$ matrix elements.

j_f	j_i	$(j_f\|\|M1\|\|j_i)$ (μ_N) 0 order	0+1st order
$\pi g_{9/2}$	$\pi g_{9/2}$	11.60	11.30
$\nu d_{5/2}$	$\nu d_{5/2}$	−2.71	−2.00
$\nu d_{5/2}$	$\nu d_{3/2}$	2.89	1.92
$\nu d_{5/2}$	$\nu g_{7/2}$	0	−0.34
$\nu s_{1/2}$	$\nu s_{1/2}$	−2.29	−1.70
$\nu s_{1/2}$	$\nu d_{3/2}$	0	−0.18
$\nu d_{3/2}$	$\nu d_{3/2}$	1.45	1.17
$\nu g_{7/2}$	$\nu g_{7/2}$	2.33	1.65

TABLE VI. Effects of the two-body graphs on the $M1$ matrix elements.

Initial state		Final state		$(J_f\|\|M1\|\|J_i)$ (μ_N) 0 order	0 order + two-body corr.
$(\pi g_{9/2})^2$	2	$(\pi g_{9/2})^2$	2	3.977	3.986
$(\pi g_{9/2})^2$	4	$(\pi g_{9/2})^2$	4	9.743	9.558
$(\pi g_{9/2})^2$	6	$(\pi g_{9/2})^2$	6	16.968	16.710
$(\pi g_{9/2})^2$	8	$(\pi g_{9/2})^2$	8	25.428	25.149
$(\nu d_{5/2})^2$	2	$(\nu d_{5/2})^2$	2	−1.535	−1.177
$(\nu d_{5/2}s_{1/2})$	2	$(\nu d_{5/2})^2$	2	0	0.183
$(\nu d_{5/2}s_{1/2})$	2	$(\nu d_{5/2}s_{1/2})$	2	−0.511	−0.105
$(\nu d_{5/2}s_{1/2})$	3	$(\nu d_{5/2})^2$	2	0	−0.036
$(\nu d_{5/2}s_{1/2})$	3	$(\nu d_{5/2}s_{1/2})$	2	1.916	1.157
$(\nu d_{5/2}s_{1/2})$	3	$(\nu d_{5/2}s_{1/2})$	3	−4.283	−4.283
$(\nu d_{5/2})^2$	4	$(\nu d_{5/2}s_{1/2})$	3	0	0.122
$(\nu d_{5/2})^2$	4	$(\nu d_{5/2})^2$	4	−3.760	−3.002

cedure described above. As may be seen from Table VII, the predictions of the two models are not very different and generally are in satisfactory agreement with experiment. This agreement is more pronounced in the cases where there is pure $E2$ decay from the initial to the final state. In the two cases, however, where there is competition between $M1$ and $E2$ modes of decay, both models overestimate the $M1$ and underestimate the $E2$ mode in comparison to experiment. As Table VII also shows, the use of effective $M1$ matrix elements produces a significant improvement to the theoretical predictions.

A final comparison between theory and experiment is made in Table VIII, where we list values of δ $(E2/M1)$ mixing ratios, branching ratios, and lifetimes. As Table VIII shows, with respect to branching ratios and lifetimes, there is an excellent agreement between the results of calculation 1 and experiment. However, this agreement is completely destroyed when one makes a comparison between the δ values obtained from calculation 1 and the experimental estimates. Thus calculation 1 produces multipole mixing ratios that are smaller in magnitude and also opposite in sign from the experimental values. It may be noticed, however, that to reproduce the signs of the two δ values from the results of calculation 1, one needs to identify the theoretical 2_2^+ state to the experimental 2_3^+ state and vice versa. Such an identification cannot be rejected on energy grounds since, as Fig. 3 shows, both the experimental and theoretical 2_2^+ and 2_3^+ states are close in energy. The results of this identification are shown in Table IX. As may be seen from Table IX, the reversal of the role of the theoretical 2_2^+ and 2_3^+ levels, apart from the sign of the two δ values, produces reasonable agreement with experiment also on the magnitude of the $\delta(E2/M1)$ ratio in the $2_3^+ \rightarrow 2_1^+$ decay. However, the agreement with experiment on branching ratios and lifetimes, although reasonable, is in this case less impressive than the one shown in Table VIII. It seems, therefore, that within the limitations of calculation 1 one cannot make a unique identification between experimental and theoretical levels.

The identification between experimental and theoretical 2^+ states presents an even greater difficulty with calculation 2. As Table VIII shows, this calculation distinguishes between 2_2^+ and 2_3^+ states only with respect to their branching ratio, since it predicts very similar $\delta(E2/M1)$ and lifetime values for both states. The predicted be-

TABLE VII. Experimental and calculated transition rates of the low-lying states of ^{94}Mo.

$J_i \rightarrow J_f$	Multipolarity	Experimental (W.u.)	Calcul. 1 (W.u.)	Calcul. 2 (W.u.)
$2_1 \rightarrow 0_1$	$E2$	17.2	19.6	22.9
$4_1 \rightarrow 2_1$	$E2$	26.6	17.0	22.9
$2_2 \rightarrow 0_1$	$E2$	$0.60^{+0.39}_{-0.48}$	0.561	0.552
$2_2 \rightarrow 2_1$	$M1$[a]	$0.09^{+0.02}_{-0.05}$	0.182	0.756
$2_2 \rightarrow 2_1$	$M1$	$0.09^{+0.02}_{-0.05}$	0.183	0.509
$2_2 \rightarrow 2_1$	$E2$	71^{+18}_{-39}	25.3	12.0
$2_3 \rightarrow 0_1$	$E2$	$1.9^{+0.6}_{-0.9}$	2.37	4.64
$2_3 \rightarrow 2_1$	$M1$[a]	$0.26^{+0.05}_{-0.10}$	0.532	0.314
$2_3 \rightarrow 2_1$	$M1$	$0.26^{+0.05}_{-0.10}$	0.402	0.238
$2_3 \rightarrow 2_1$	$E2$	71^{+37}_{-39}	4.62	5.19

[a] Bare operator.

TABLE VIII. Experimental and calculated electromagnetic properties of the low-lying states of ^{94}Mo.

		Experiment			Calculation 1			Calculation 2		
J_i	J_f	$\delta(E2/M1)$	Branch %	Tm (ps)	$\delta(E2/M1)$	Branch %	Tm (ps)	$\delta(E2/M1)$	Branch %	Tm (ps)
2_1^+	0_1^+		100	3.7 ± 0.02		100	3.19		100	2.73
4_1^+	2_1^+		100	7.1 ± 1.0		100	10.8		100	8.03
2_2^+	0_1^+		8			6.2			1.6	
				$0.185^{+0.09}_{-0.04}$			0.155			0.065
	2_1^+	$-0.87^{+0.09}_{-0.17}$	92		0.369	93.8		0.148	98.4	
2_3^+	0_1^+		10			11.3			29.4	
				0.046 ± 0.01			0.040			0.053
	2_2^+	$0.62^{+0.21}_{-0.15}$	90		−0.128	88.7		0.176	70.6	

havior, however, is exactly the opposite of that experimentally observed, which is also shown in Table VIII. This situation is not significantly improved by an inversion in the identification of the two 2^+ theoretical states, similar to the one discussed in relation with calculation 1, due to the proximity in the energies of the two levels.

One may conclude that the predictions of calculation 1 on the decay of the low-lying states of ^{94}Mo are in closer agreement with experiment than those of calculation 2. This result certainly reflects the lack of detailed mixing between neutron configurations in the wave functions of calculation 2.

It is evident from the above discussion that there is ground for further theoretical investigation on the low-lying levels of ^{94}Mo. From the two models employed here calculation 1 produces better agreement with experiment on transition rates, while calculation 2 can account for all the observed levels. A merge of the two model spaces appears to be the natural starting point for a more extended calculation. Certainly the need for such an extended calculation will become stronger when

TABLE IX. Alternative description of the decay of the second and third 2^+ states of ^{94}Mo.

		Experiment			Calculation 1a		
J_i	J_f	$\delta(E2/M1)$	Branch %	Tm (ps)	$\delta(E2/M1)$	Branch %	Tm (ps)
2_2^+	0_1^+		8			11.8	
				$0.185^{+0.09}_{-0.04}$			0.069
	2_1^+	$-0.87^{+0.09}_{-0.17}$	92		−0.106	88.2	
2_3^+	0_1^+		10			5.3	
				0.046 ± 0.01			0.079
	2_1^+	$0.62^{+0.21}_{-0.15}$	90		0.444	94.7	

further experimental information becomes available on ^{94}Mo. Of particular interest would be information on the decay rate of the second 0^+ level of ^{94}Mo, recently established to be at 1.74 MeV,[23] and on the feeding of the higher levels of ^{94}Mo to the ones discussed here. Such information might also make the identification between experimental and theoretical levels more obvious.

[1]C. A. Kalfas, A. C. Xenoulis, E. Adamides, S. Papaiannou, and L. D. Skouras, Z. Phys. A 292, 153 (1979).
[2]N. K. Aras, E. Eichler, and G. G. Chilosi, Nucl. Phys. A112, 609 (1968).
[3]J. Barrette, M. Barrette, A. Boutard, R. Haroutinian, G. Lamoureux, and S. Monaro, Phys. Rev. C 6, 1339 (1972).
[4]N. Cue, I. Plesser, Z. Vager, and G. F. Wheeler, Nucl. Phys. A229, 429 (1974).
[5]W. Hauser and H. Feshbach, Phys. Rev. 87, 366 (1952).
[6]E. Sheldon and R. M. Strang, Comp. Phys. Commun. 1, 35 (1969).
[7]G. S. Mani, M. Malkenoff, and I. Lori, Saclay Report No. CEA 2379, 1963 (unpublished).
[8]F. James and M. Roos, CERN Library, Report No. B506, 1971 (unpublished).
[9]M. S. Zisman, F. D. Becchetti, B. G. Harvey, D. G. Kovar, J. Mahoney, and J. D. Sherman, Phys. Rev. C 8, 1866 (1973); T. Wada, Nucl. Phys. A307, 425 (1978).
[10]D. W. O. Rogers, Nucl. Instrum. Methods 127, 253 (1975).
[11]K. S. Krane and R. M. Steffen, Phys. Rev. C 2, 724 (1970).
[12]D. C. Kocher, Nucl. Data Sheets 10, 241 (1973).
[13]C. Moazed, T. Becker, P. A. Assimakopoulos, and D. M. Van Patter, Nucl. Phys. A169, 651 (1971).
[14]L. Lindhard, M. Scharff, and H. E. Schiøtt, K. Dan. Vidensk. Selsk. Mat.-Fys. Medd. 33, No. 14 (1963).
[15]A. E. Blaugrund, Nucl. Phys. 88, 501 (1966).
[16]D. G. Sarantites, J. H. Barker, N. H. Lu, E. J. Hoffman, and D. M. Van Patter, Phys. Rev. C 8, 629 (1973).
[17]C. Dedes and L. D. Skouras, Phys. Lett. 66B, 417 (1977).
[18]L. D. Skouras and C. Dedes, Phys. Rev. C 15, 1873 (1977).
[19]J. P. Elliott, A. D. Jackson, H. A. Mavromatis, E. A. Sanderson, and B. Singh, Nucl. Phys. A121, 241 (1968).
[20]J. D. Vergados and T. T. S. Kuo, Phys. Lett. 35B, 93 (1971).
[21]D. H. Gloeckner and F J. D. Serduke, Nucl. Phys. A220, 477 (1974).
[22]D. H. Gloeckner Nucl. Phys. A253, 301 (1975).
[23]Y. Sugiyama and S. Kikuchi, Nucl. Phys. A264, 179 (1976).
[24]A. Arima and H. Horie, Prog. Theor. Phys. 11, 509 (1954); 12, 623 (1954).